Progress In Electromagnetics Research Letters, Vol. 94, 67–73, 2020

Miniaturized Triple-Section Spiral Antenna with Improved Radiation

Guangyao Yang[1, 2], Shengbo Ye[1, *], Yicai Ji[1, 2], Xiaojuan Zhang[1], Guangyou Fang[1, 2]

Abstract—A triple-section arm structure is proposed for designing a planar spiral antenna. All three sections are designed by combining logarithmic, rooted, and sine equations. The slowly outstretched and contractive structure is innovatively realized. According to the radiation characteristics of the spiral antenna, each section corresponds to different in-band enhancement effects. Numerical simulation in the frequency domain and experiments using two different baluns are carried out. The results show that the novel spiral topology could simultaneously achieve improved axial ratio, low cross-polarized gain, and excellent impedance matching throughout the whole band. The axial ratio is reduced by 1.5 dB at mid-frequencies and more at low frequencies, comparing the proposed arm with a sinusoid-added equiangular spiral arm. Without applying the resistive loading method, a lower cut-off frequency of 750 MHz is still realized both in impedance bandwidth and axial ratio bandwidth. The low cut-off frequency of the proposed arm is 30.2% lower than the conventional Equiangular spiral arm. Besides, the polarization isolation is significantly improved, especially at low frequencies. Therefore, the proposed miniaturized spiral arm structure could be a competitive form for designing spiral antennas.

1. INTRODUCTION

In many commercial and military applications, broadband antennas with circularly polarized (CP) radiation characteristics are needed. Spiral antennas have flat input impedances, stable gains, and standard circular polarization patterns over multi-octaves band. Spiral antennas have been widely used for ultra-wideband (UWB) applications, such as communications, radar, and navigation. However, spiral antennas of simple form have larger profiles, worse axial ratio, and lower gain when being operated at low frequencies. In the past, much research has been done to enhance the performances of traditional spiral antennas. Loading methods, such as dielectric loading, inductive loading, and resistive loading, have been proposed to design several spiral antennas [1–4]. The electromagnetic wavelength could be shortened by burying the metal wire into the dielectric substrate [1]. The current path could be stretched by coiling the spiral arm [2, 3]. Current reflections at the end of the spiral arm could be further suppressed by applying a lossy termination [4]. Finally, the loaded spiral antenna could be miniaturized. In addition to the loading method, new arm structures have also been designed to improve the inherent performance of Archimedean spiral and equiangular spiral [5–7]. The equation of the arm is totally rewritten or simply added in a power factor to create novel current paths [5]. Different spiral forms can be combined to get over weaknesses in different spiral parts [6]. New arms with advanced equations are expected to solve the conventional disadvantages and endow the spiral antennas with better performances.

In this paper, a novel arm structure with gradient inductive loading is proposed for spiral antenna, as shown in Fig. 1. The arms are etched on the single layer and can be separated into three novel sections. The equation of each section is specially designed by integrating theory-based experience. The

Received 10 August 2020, Accepted 21 October 2020, Scheduled 25 October 2020

* Corresponding author: Shengbo Ye (shengboye@163.com).

[1] Key Laboratory of Electromagnetic Radiation and Sensing Technology, Aerospace Information Research Institute, Chinese Academy of Sciences, Beijing 100190, China. [2] University of the Chinese Academy of Sciences, Beijing 100039, China.

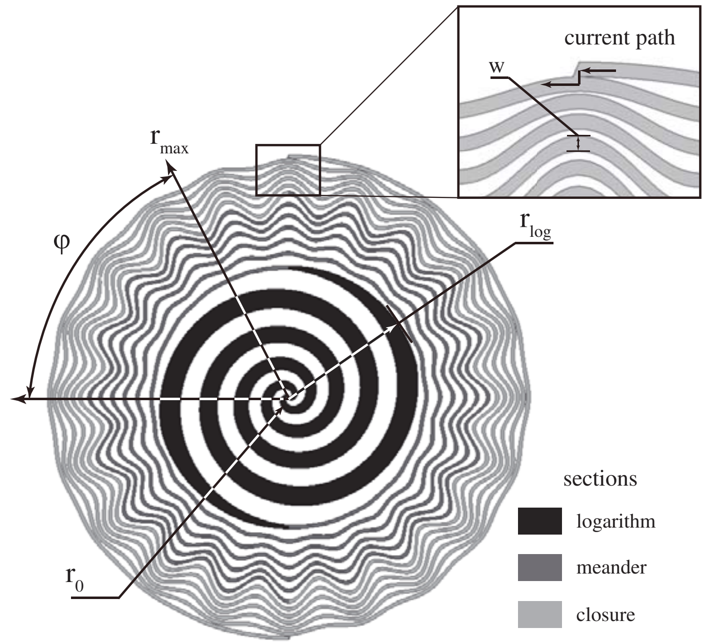

Figure 1. Proposed spiral arm structure.

first logarithm-section is totally self-complementary and aims to realize a wideband low axial ratio. The second meander-section aims to reduce the low cut-off frequency. Lifting axial ratio at low frequency is ameliorated by the third closure-section. A long exponential tapered balun and a shortened wideband Chebyshev stepped balun operating in L/S band are also designed for antenna tests. Simulated and experimental results confirm the effectiveness of the spiral arm design.

2. GEOMETRY OF TRIPLE-SECTION ARM

The configuration of the proposed spiral antenna is illustrated in Fig. 1. The arm structure composed of three sections is shown in three colors. The first center part is connected by two logarithm equations written as,

$$r = a\varphi_1 \cdot \ln(1 + b\varphi_1) \tag{1}$$

$$r = a(\varphi_2 + \pi/2) \cdot \ln[1 + b(\varphi_2 + \pi/2)] \tag{2}$$

Eqs. (1) and (2) describe the inner edge and outer edge, respectively. The ranges of rotating angles φ_1 and φ_2 that represent the true angles in polar coordinates are defined as $\varphi_1 \in [\pi/4, n]$ and $\varphi_2 \in [-\pi/4, n]$. The growth rate of the proposed arm is controlled by parameters a and b. Note that the growth rate is boosted slowly along with increase of the rotating angle. This special feature fits with the total arm structure. The self-complementary topology is achieved within the circle with a radius $r_{\log}$. Compared with a conventional exponential arm, the logarithmic spiral arm could achieve a lower axial ratio. Meanwhile, the flat impedance curve and similar gain are also maintained. The related results will be shown and analyzed later. This region mainly radiates high-frequency spectral components.

As shown in recent research, the axial ratio at low frequencies improves with increased coupling between the spiral arms in the active region, which is caused by the tighter wrapping near the antenna's perimeter. The width of the arm around $r_{\log}$ converges to w. Then this line enters a growing meandering area, called meander-section. The equation follows as,

$$r = c\varphi^{\frac{1}{2}} \cdot \{1 + m \ln[1 + (\varphi - n)/(n_1 - n)] \cdot \sin(e\varphi + \pi/2)\} \tag{3}$$

The value of parameter c is around 7.74, which ensures the connection between the first two sections. The rotating angle φ of the Archimedean spiral is added with a root power to increase arm coupling. Another logarithmic part with parameter m is introduced to control the growth of meandering. Parameter e influences the number of meandering periods from n to n_1. Thus, the minimum cut-off frequency is determined together by m and e.

To avoid the deterioration of the axial ratio at the low-frequency spectrum, the meandering must demise gradually. Then the additional part with parameter p is proposed to recover a flat circle. The root power ensures a tight coupling even when the sinusoidal trend is reduced. The equation of closure-section is designed as,

$$r = c\varphi^{\frac{1}{2}} \cdot \{1 + m \ln\left[1 + (\varphi - n) / (n_1 - n) - p \cdot (\varphi - n_2)/(n_1 - n_2)\right] \cdot \sin(e\varphi + \pi/2)\} \tag{4}$$

At the angle of n_2, the two arms are shorted to obtain a better performance. Residual current at the perimeter is guided into another arm to radiate more standard CP wave. From n to n_2, the growth rate of the spiral is decreased slowly. A novel smooth transition from the growth rate to the declining rate is then achieved. After a reasonable parameter setting, the two arms of the proposed antenna are kept very close to each other without intersecting. The values of parameters mentioned above are listed in Table 1, which have already been optimized by Ansys HFSS. For further understanding of the physical meanings of the parameters, see Appendix A.

Table 1. Structure parameters of proposed spiral arm.

Parameters	Value	Parameters	Value
a	0.002	r_0	2 mm
b	0.1	$r_{\log}$	30.67 mm
w	1 mm	$r_{\max}$	55 mm
m	0.08	n	5π
e	20	n_1	11π
p	1	n_2	17π

3. RESULTS AND DISCUSSION

The fabricated prototype with a detailed view and backward view is shown in Fig. 2(a). To test the proposed spiral arm, two baluns are designed to feed the differential signal to the fabricated prototype. The proposed arms are etched on FR-4 with 1 mm thickness, while Rogers 4350B with 0.762 mm is

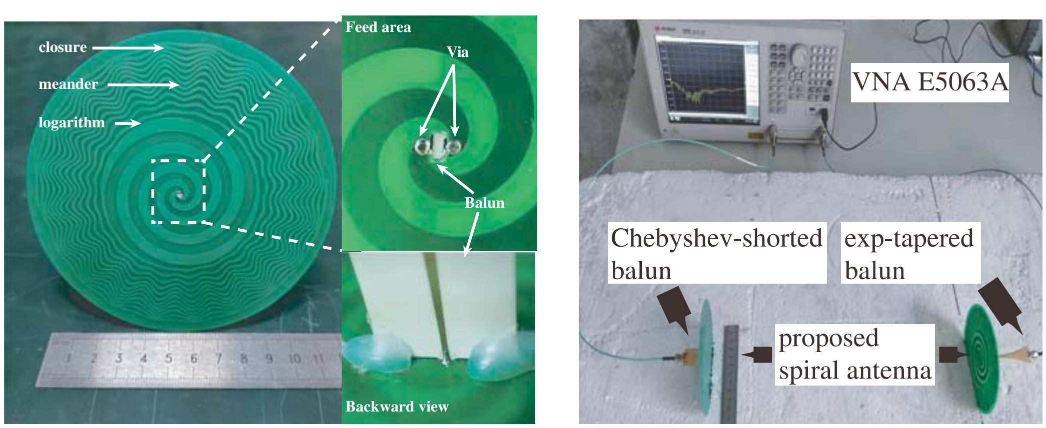

(a) (b)

Figure 2. (a) The fabricated antenna. (b) The test scene with fabricated antenna and different baluns.

chosen to be the substrate of baluns. The first balun is a traditional exponential-tapered balun, which transforms 50 Ω microstrip (MS) line to 100 Ω double-sided parallel-strip line (DSPSL). The total length is 90 mm to realize a low cut-off frequency under 700 MHz. The first balun has better performance, but its oversized profile limits the application. The second 36 mm balun is much shorter than the former one. The 50 Ω coaxial cable connects the coplanar waveguide (CPW). Then the impedance is transferred to 100 Ω by five Chebyshev stepped tapers. Through grounded-CPW (GCPW) and MS line to DSPSL, the electric field is balanced. The test scene including the proposed fabricated triple-section spiral antenna (TSS) and two baluns are shown in Fig. 2(b). All measured results are recorded by a vector network analyzer (VNA) numbered Keysight E5063A.

The simulated and measured VSWR results, as well as the structure of the two baluns, are shown in Fig. 3. Despite the effects of baluns, the results achieve the same trend in curves. The simulated VSWR bandwidth starts from 700 MHz, while the measured results of TSS with the long exponential-tapered balun and Chebyshev-shorted balun are 750 MHz and 760 MHz, respectively. The impedance at the low band is influenced by the fabricating precision. As the arms wrap tightly at the perimeter, the shortest distance between them is around 1 mil. The minimum processing tolerance is 5 mil, so the sine shape around the final lap is slightly pared. Connected with baluns, the measured results of fabricated TSS are worse than the simulated one, but the effectiveness of the design is still remarkable. For comparison, a conventional Logarithmic spiral (Equiangular spiral, ES) with the same diameter is also simulated. The obtained VSWR result is shown in Fig. 3. The measured low cut-off frequency of the proposed spiral arm in terms of impedance matching is 30.2% lower than the conventional ES arm, of which the maximum perimeter is almost the wavelength corresponding to the lowest operating frequency.

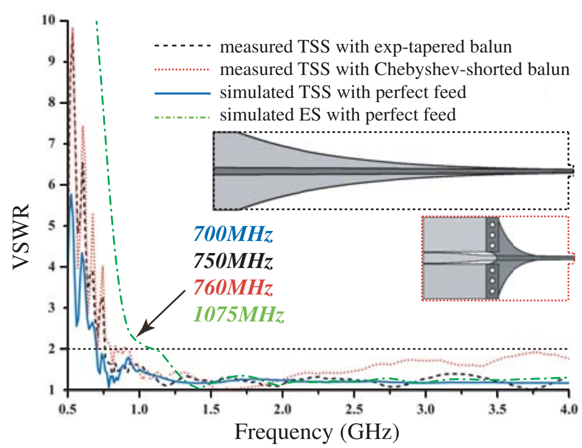

Figure 3. The VSWR results of ES and TSS with different feeds.

To illustrate more advantages of the proposed antenna, a typical equiangular spiral terminated with sine meander-section (MES) is simulated for comparison. Along with the conventional ES, the three spiral structures have the same maximum diameter and substrate. The equidistance wrapping surely broadens the impedance bandwidth of MES, but it cannot expand the axial ratio (AR) bandwidth well, so do most traditional spiral arms. The simulated AR results of ES, MES, and TSS at the lower band (slash fill region) are compared in Fig. 4(a). Without loading and proper outer arm design, the conventional ES radiates elliptical polarization. However, the proposed TSS represents a noticeably better AR. In addition to the perfect performance at low cut-off frequency, the AR at higher frequencies is also reduced up to 1.5 dB compared to MES. In Fig. 4(b), simulated and measured AR results of TSS are shown. The longer balun is used for AR measurement. The measured result is almost consistent with the simulated one, except for the part at the low-end frequency. This result verifies the influence of fabricating precision mentioned above.

The realized gains of ES, MES, and TSS are compared in Fig. 5. The three spirals radiate right-hand circularly polarized (RHCP) waves at boresight direction. The conventional ES cannot be operated at frequencies lower than 2 GHz, so the realized gain is lower than the other two spirals. Meanwhile, the

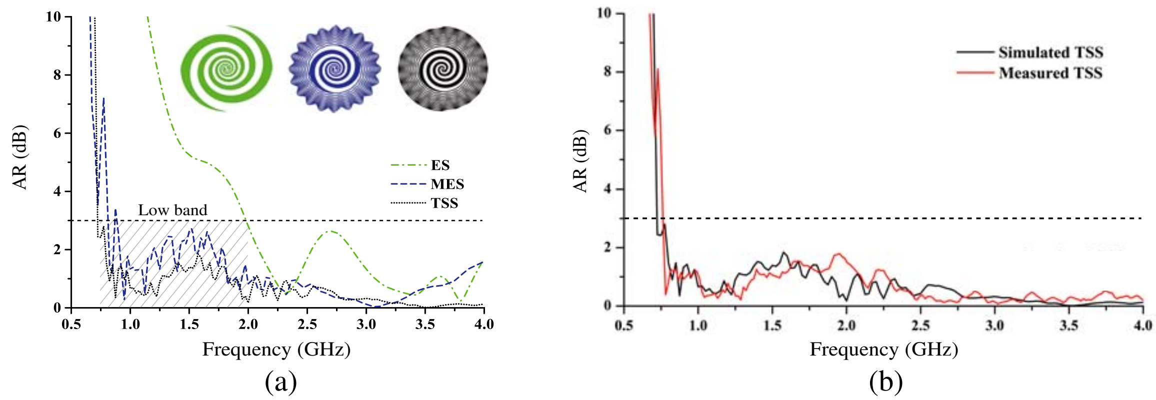

Figure 4. (a) The comparison for ARs of ES, MES, and TSS. (b) Simulated and measured ARs of TSS.

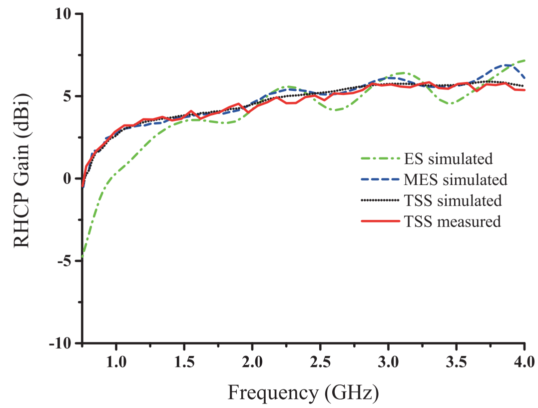

Figure 5. The comparison for RHCP gains of ES, MES, and TSS.

reflection from the end makes its gain fluctuate at higher frequencies. The TSS shows a comparable co-polarized gain with the MES at the whole band, but the increasing trend is more stable. The measured co-polarized gain of the proposed TSS is also shown in Fig. 5 with a red solid line. The simulated and measured results are basically consistent.

Apart from the axial ratio, polarization isolation is also a critical radiation performance for the spiral antenna. Fig. 6 shows the simulated radiation pattern of the two spirals. Similar main polarized (RHCP) patterns can be seen at 0.75 GHz, 1 GHz, 2 GHz, and 4 GHz. However, significant differences occur in the cross-polarized (LHCP, see Appendix A) patterns. At all frequencies, the TSS maintains a much smaller cross-polarized gain at boresight than conventional ES. Especially at low cut-off frequency, the isolation value is higher than 17.5 dB, while the ES with two sections only achieves 10 dB. Hence, the proposed TSS is more suitable for polarization diversity application scenarios. For radar applications, the characteristics of low AR and high polarization isolation also help to distinguish different targets. Therefore, the proposed TSS can be an efficient tool for practical radio applications.

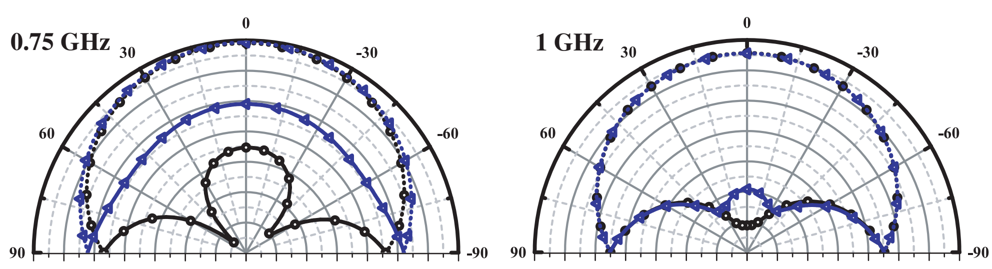

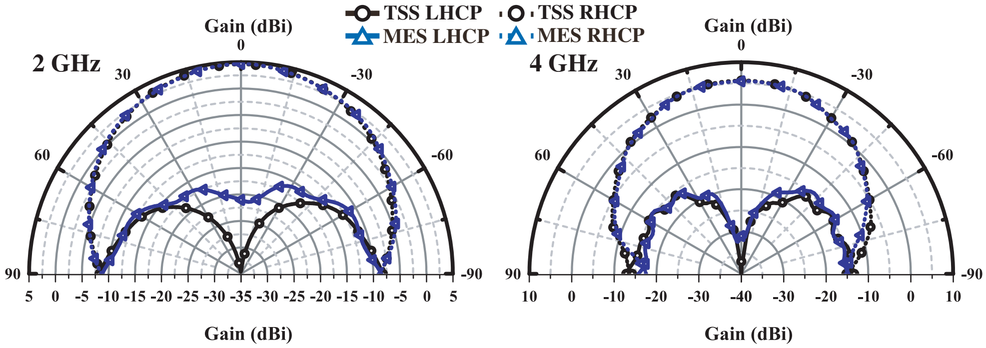

Figure 6. The LHCP/RHCP patterns of MES and TSS.

4. CONCLUSION

A novel uniplanar spiral structure with a triple-section arm is presented in this paper. Each section follows a different novel equation and realizes multiple improvements. A novel frequency-independent spiral structure with the self-complementary characteristic is formed by inner logarithm curves. A gradual sine curve is generated by mathematical analysis. Finally, it is verified that the impedance bandwidth and the axial ratio bandwidth obtain the same starting frequency. The miniaturization of the spiral antenna is realized, and the polarization isolation is promoted.

ACKNOWLEDGMENT

This research work is supported in the National Key Research and Development Plan 2017YFC0822100 and Beijing Municipal Science and Technology Commission Z181100000118004.

APPENDIX A. NOMENCLATURE

List of Parameters and Acronyms

a	total growth rate of the logarithm	AR	axial ratio
b	growth factor of angel	CP	circularly polarized
c	compensation factor of the proposed arm	CPW	coplanar waveguide
e	angular velocity of gradient sine	DSPSL	double-sided parallel line
m	growth factor of gradient sine	ES	equiangular spiral
n	maximum angle of the logarithm-section	GCPW	grounded coplanar waveguide
n_1	maximum angle of the meander-section	LHCP	left-hand circularly polarized
n_2	maximum angle of the total arm	MES	meandered equiangular spiral
p	descending factor of gradient sine	MS	microstrip
r_0	minimal radius of the proposed arm	RHCP	right-hand circularly polarized
$r_{\log}$	transition radius of the proposed arm	TSS	triple-section spiral
$r_{\max}$	maximum radius of the proposed arm	UWB	ultra-wideband
w	width of the meadering line	VNA	vector network analyzer
		VSWR	voltage standing wave ratio

REFERENCES

1. Obrien J. M., J. E. Grandfield, G. Mumcu, et al., "Miniaturization of a spiral antenna using periodic Z-plane meandering," *IEEE Trans. Antennas Propag.*, Vol. 63, No. 4, 1843–1848, 2015.
2. Kramer, B. A., C.-C. Chen, and J. L. Volakis, "Size reduction of a low-profile spiral antenna using inductive and dielectric loading," *IEEE Antennas Wireless Propag. Lett.*, Vol. 7, No. 7, 22–25, 2008.
3. Volakis,J. L., C.-C. Chen, and K. Fujimoto, *Small Antennas: Miniaturization Techniques and Applications*, McGraw-Hill, New York, NY, USA, 2010.
4. Shih, T. and N. Behdad, "A compact, broadband spiral antenna with unidirectional circularly polarized radiation patterns," *IEEE Trans. Antennas Propag.*, Vol. 63, No. 6, 2776–2781, 2015.
5. Elmansouri M. A. and D. S. Filipovic, "Low-dispersion spiral antennas," *IEEE Trans. Antennas Propag.*, Vol. 60, No. 12, 5522–5530, 2012.
6. Ranjbaran S. M. H. and S. Mohanna, "Improved spiral antenna with a new semi-fractal reflector for short-range sensing," *IET Microw. Antennas Propag.*, Vol. 12, No. 11, 1839–1845, 2018.
7. Sharma C. and D. K. Vishwakarma, "Miniaturization of spiral antenna based on fibonacci sequence using modified koch curve," *IEEE Antennas Wireless Propag. Lett.*, Vol. 16, 932–935, 2017.